Research Article

Effect of Time Stepping in the Filtering Process on the Synthesis of Nickel Sulfate Powder from Blast Furnace Ferronickel

Aprilio Muhammad Fulesa, Yuli Setiyorini, Fakhreza Abdul and Sungging Pintowantoro*
Department of Materials and Metallurgical Engineering, Faculty of Industrial Technology and System Engineering, Institut Teknologi Sepuluh Nopember, Surabaya, Indonesia

* Corresponding author. E-mail: sungging@mat-eng.its.ac.id
DOI: 10.14416/j.asep.2023.06.002
Received: 2 April 2023; Revised: 30 April 2023; Accepted: 16 May 2023; Published online: 23 June 2023

Abstract

The demand for nickel manganese cobalt (NMC)-type batteries is increasing along with the need for global electric vehicles, such as electric cars. Nickel used in the manufacture of NMC batteries is Nickel (II) sulfate hexahydrate ($NiSO_4.6H_2O$). Therefore, it is necessary to study how to synthesize nickel sulfate powder from blast furnace ferronickel to provide an alternative source of nickel sulfate and increase the added value of blast furnace ferronickel products. This study aims to analyze the effect of variations in the time difference of stepped filtering sludge on the precipitated filtrate. This study uses a nickel source from the ferronickel derived from the sintering and smelting process using a Mini Blast Furnace to synthesize nickel sulfate. First, the ferronickel was ground and sieved to pass 50 mesh size. Then, the leaching process was performed using a mixture of 120 mL H_2SO_4 (2M) and 30 mL H_2O_2 (30%) with a stirring speed of 200 rpm for 6 h for each 2 g ferronickel. Next, the precipitation process was carried out using $CaCO_3$ powder to pH 3.01 at 90 °C. The precipitation solution was held at 90 °C for 24 h, and stepped filtering of the precipitate formed with variations of 2, 4, 6, and 8 h (the total time is kept the same, i.e., 24 h). The crystallization results were then washed and dried at 70 °C for 2 h. Based on X-Ray Fluorescence (XRF), the best results were obtained in stepped filtering variation every 8 h with 50.23% Ni content and 90.5% Ni separation efficiency. Based on XRD, the nickel sulfate powder product has the compound $NiSO_4.6H_2O$. In addition, nickel sulfate products also contain $CoSO_4$, one of the compounds needed to manufacture NMC batteries. However, nickel sulfate powder products still contain impurity compounds like $FeSO_4$ and $CaSO_4$.

Keywords: Ferronickel, Batteries, Separation, Precipitation, $NiSO_4.6H_2O$

1 Introduction

One hundred ninety-five countries agree upon the Paris Agreement to maintain a maximum increase in global temperature of 2 °C [1]. At the same time, Battery Electric Vehicles (BEVs) have low CO_2 emissions [2]. The battery is an essential component in the Battery-Electric Vehicle and functions as a store of electrical energy, which is later converted into mechanical energy. The battery used in electric vehicles is lithium-ion. Of the various types of lithium-ion batteries, Nickel Manganese Cobalt (NMC) batteries have the most superior properties to be applied to electric vehicles because they have high energy density and life cycle [3]. NMC cathode was synthesized by using hydroxide coprecipitation and calcination process. The components used are sulfate compounds, namely $NiSO_4.6H_2O$, $MnSO_4.H_2O$, and $CoSO_4.7H_2O$ [4]. As an essential material in the manufacture of NMC batteries, the demand for nickel production will also increase [5]. In this study, laterite nickel processing begins with smelting using Mini Blast Furnace (MBF). It aims to reduce and smelt laterite nickel into ferronickel. In ferronickel, several other elements exist, such as iron (Fe) and cobalt (Co). Then the ferronickel is followed by a hydrometallurgical process.

Hydrometallurgy is a method for extracting metals from their ores by dissolving them into solutions [6]. There are two main processes in hydrometallurgy: leaching and separation [6]. Several factors affect the leaching, such as temperature, reactant concentration, liquid-solid ratio, pH, and the leaching time [7]. After the leaching is complete, a solution with a high acidity level is obtained, and it is necessary to carry out a precipitation process [8]. Precipitation of other elements by adding a precipitating agent is an excellent method to obtain nickel products with good recovery [9]. In the nickel laterite precipitation process, several compounds or agents are commonly used, one of which is $CaCO_3$, because of its low cost and can be used for iron precipitation [10].

However, adding $CaCO_3$ also has a drawback, namely the formation of $CaSO_4$ as a new impurity [10]. Another additive that can be added to introduce precipitation of impurities in the leaching solution is NaOH [11]. Other methods to reduce impurities from the leaching solution are magnetic seeding to reduce iron content in the solution [12], the addition of limonite seeding to remove iron through goethite precipitation [13], the addition of ozone as an oxidizing agent to produce Co and Mn precipitates [14]. Impurities will affect some battery performance, electrochemical performance, stability, and lifetime [15]. For NMC battery grades, the maximum tolerated Ca impurity is 0.01 wt% [15].

However, reducing impurities in leaching solutions by adding alkaline additives is a simple method, even though the selectivity could be higher [16]. So that after the precipitation process, it is necessary to do post-treatment to reduce impurities. A heating and stepped filtering process was carried out to increase the metal saturation before crystallization. Crystal washing was carried out to obtain good-quality $NiSO_4.6H_2O$ crystals and minimize the $CaSO_4$ impurities. This study aims to analyze the effect of variations in the time difference of stepped filtering on the precipitated filtrate.

2 Materials and Method

2.1 *Materials*

2.1.1 Ferronickel

The samples used in this study were ferronickel products obtained from the sintering and smelting process in the Mini Blast Furnace, as we have done in our previous research [17], [18]. Atomic Absorption Spectroscopy (AAS) testing was carried out on ferronickel. It was performed to determine the elemental composition contained in crude ferronickel. The following are the results of the AAS testing of crude ferronickel contained in Table 1.

2.1.2 Leachate filtrate

After the ferronickel leaching process, AAS characterization was also carried out to obtain information related to the elemental contentment in the leachate. The outcome of the AAS test of ferronickel leachate can be seen in Table 1.

2.1.3 Solution after precipitation process

Samples resulting from the precipitation of the leachate were also tested using AAS to examine the elemental composition. The appearance of Ca in the solution is due to the precipitation process carried out using $CaCO_3$, so there is quite a lot of Ca content in the solution. Table 1 shows the results of the AAS test for the precipitated solution.

Table 1: Chemical composition of materials in this research based on AAS analysis

Sample	Metal Content (wt%)			
	Ni	Fe	Co	Ca
Crude Ferronickel	33.92	71.82	0.94	-
Leachate	32.27	66.76	0.97	-
Precipitated solution	89.20	2.30	0.81	7.69

2.2 *Method*

2.2.1 Materials preparation

The sample used is ferronickel from ore from Southeast Sulawesi, which has been smelted using a mini blast furnace at the Department of Materials and Metallurgical Engineering, ITS, Surabaya. First, Ferronickel was ground and sized. The ferronickel powder had a homogeneous size of (-) 50 mesh. It was done to speed up the leaching process because a more extensive contact area of the metal particles with leachate causes higher material transfer. Then, four samples of ferronickel were weighed with a mass of 2 g each.

2.2.2 Leaching process

The leaching process aims to dissolve the elements in the ferronickel sample. The leaching was carried out using 120 mL of 2M sulfuric acid solution and 30 mL of H_2O_2 30%. The leaching was carried out for 6 hours with a fixed variable: a stirring speed of 200 rpm and a temperature of 90 °C. These conditions were selected based on our previous research [19], [20]. After the leaching was complete, filtering was carried out using filter paper to separate the filtrate and residue from the leaching. The AAS characterized the leaching filtrate (leachate) to obtain the concentration of metal contained after extraction/leaching. The reaction resulting from reacting hydrogen peroxide acid and sulfuric acid on ferronickel is shown in Equations (1) and (2), where M is either Ni, Co, or Fe.

$$M_{(s)} + H_2O_{2(aq)} \rightarrow MO_{(s)} + H_2O_{(l)} \qquad (1)$$

$$MO_{(s)} + H_2SO_{4(aq)} \rightarrow MSO_{4(aq)} + H_2O_{(l)} \qquad (2)$$

2.2.3 Precipitation process

In this research, the precipitation process used $CaCO_3$ powder. Precipitation was performed until the pH reached 3.01. Then, a pH meter was used to measure the pH of the solution. The addition of $CaCO_3$ powder was gradually carried out through several trials to control the pH of the solution. Then, the filtrate/solution was filtered and detached from the precipitate using filter paper. Finally, the precipitation filtrate was tested by AAS to determine the metal concentration present after the precipitation process.

2.2.4 Stepped filtration process

Post-treatment was performed for precipitated filtrate by stepped filtration during the heating process to maximize the deposition of impurities. The heating process was carried out at 90 °C for 24 h. When the heating process occurs, stepped filtration is carried out. The stepped filtering process was carried out using filter paper with variations in the filtering time, namely, 2, 4, 6, and 8 h.

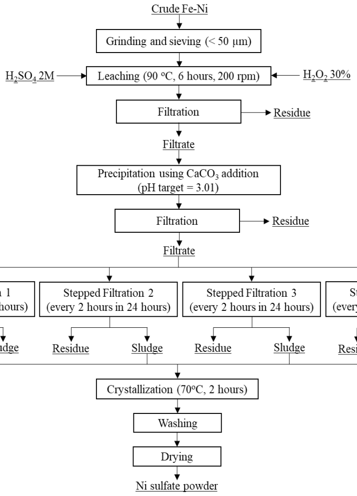

Figure 1: Research method flowchart.

2.2.5 Crystallization and washing process

The crystallization process was carried out to obtain crystals from the post-treatment. The crystallization process was carried out at 70 °C for 2 h. Then the mass of crystals formed was weighed using an analytical balance. The washing process aims to separate nickel sulfate crystals that are soluble in distilled water from crystals of impurity compounds that are not soluble in distilled water. The washing process is done by dissolving nickel sulfate crystals with distilled water in a ratio of 1 g of crystals/10 mL of distilled water and then filtering using filter paper to separate the filtrate and residue from the washing process. The filtrate from the washing process was re-crystallized at 70 °C for 2 h. The product of the crystallization process is then weighed. Next, the crystals were characterized using XRF and XRD. The flowchart of the research method is shown in Figure 1.

2.3 *Calculation*

In this study, XRF and AAS were tested on ferronickel. The XRF and XRD characterization were performed for the crystal product. Furthermore, the AAS characterization was also performed for leachate, precipitation filtrate, and filtrate from heating and stepped filtration after precipitation. The results of this AAS test are then used as the basis for calculating recovery. The calculation of recovery can be done using Equation (3) [21].

$$\%Recovery = \frac{Metal\ content\ in\ product \times Product\ mass}{Metal\ content\ in\ sample \times Sample\ mass} \times 100\% \quad (3)$$

In addition to recovery, a calculation of Separation Efficiency was also performed. Separation Efficiency calculation is carried out to determine which process is better even though each variation has differences in grade and recovery. Separation Efficiency can be defined by Equation (4) [21].

$$Separation\ Efficiency = \frac{100\ .C\ .m\ .\ (c-f)}{(m-f)\ .f} \quad (4)$$

Where, c is the percentage of precious metals in the product, f is the percentage of precious metals in the feed, m is the percentage of precious metals in the valuable feed minerals, and C is a ratio of product weight to feed weight.

3 Results and Discussion

3.1 *Effect of time of stepped filtering sludge on concentration Fe, Ni, Co, and Ca in solution*

The effect of variations in the time difference of stepped filtering when heating on the solution concentration can be seen from the AAS test. The result can be seen in Table 2.

Table 2: AAS Test result of stepped filtration filtrate

Stepped Filtration Time	Metal Content (wt%)			
	Ni	Fe	Co	Ca
2 h	93.66	0.96	0.86	4.52
4 h	91.60	0.94	0.95	6.51
6 h	91.59	0.85	0.92	6.63
8 h	91.30	0.76	0.84	7.10

In the precipitation process, a precipitating agent ($CaCO_3$) was added to precipitate impurities to obtain nickel products with good recovery. A precipitate can be formed when a solution reaches its saturation point. However, based on Table 2, there are still impurities in the form of Fe, Co, and Ca from the precipitation process results. Therefore, a heating process was carried out at 90 °C for 24 h to remove impurities in the precipitation filtrate. The heating process in the precipitation filtrate can increase the solubility of impurities so that, in the process, the impurities will settle [22].

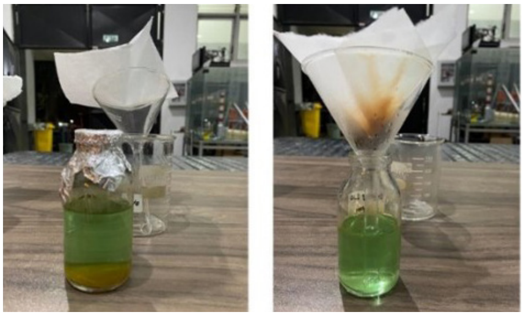

Figure 2: Sludge filtering process.

At the initial heating stage, the clear filtrate becomes more turbid as time increases. Over time, a light brown precipitate will be formed at the bottom of the filtrate container bottle, which is $FeCO_3$ because of the previous precipitation process. As the heating continues, the Ca in the solution will be precipitated into $CaSO_4$ compounds [23]. The $CaSO_4$ precipitate can not be visually seen because it is a very fine crystal seed mixed with the $FeCO_3$ precipitate. Then the precipitate formed is filtered with four variations of the difference in filtering time. Finally, the precipitate filtering process is carried out using filter paper which can be seen in Figure 2.

During 24 h of heating, there were four variations in the time difference for sludge filtering, namely 2, 4, 6, and 8 h. In a supersaturated solution, a dynamic equilibrium occurs, where a precipitate will continue to form, and at the same time, there is a dissolved precipitate. Therefore, when filtering is carried out, the equilibrium will shift. It follows Le Chatelier's Principle: If a system at equilibrium is disturbed, it responds to counter the disturbance and reestablish equilibrium [24]. When filtering the precipitate, there will be a change in solute to solvent ratio, so the equilibrium will shift. The system will react by forming a precipitate again if the solution has a solute greater than its equilibrium point. It is what causes the results of the AAS test on the precipitation filtrate in Table 2. The smaller the difference in filtering time, the more impurities are reduced, so the Ni percentage can increase. The stepped sludge filtering process is proven to reduce the content of impurities of Fe.

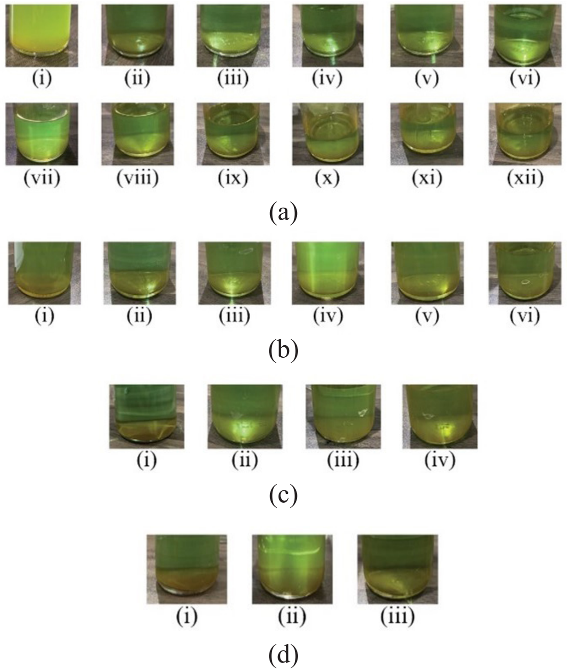

Figure 3: Sludge on stepped filtration with a time variation of (a) 2, (b) 4, (c) 6, and (d) 8 h.

On the other hand, the Ca content in filtrate was increasing. Based on this, it appears that the stepped filtering process is only effective in reducing iron content in the solution compared to calcium. It happens because the addition of $CaCO_3$ allows the reaction between $FeSO_4$ in the filtrate with $CaCO_3$ to form $CaSO_4$ and $FeCO_3$. The solubility of $FeCO_3$ in water is much lower than that of $CaSO_4$. Therefore, it makes it easier for iron compounds to form precipitates and be filtered out in the stepped filtration process. While $CaSO_4$ remains dissolved in the filtrate after filtration.

The solution concentration with the highest nickel content was obtained by varying the time of gradual sediment filtration for 2 h with a nickel content of 93.66%. Every time the filtering occurs, the equilibrium shifts towards forming a precipitate. The precipitate formed due to the influence of the stepped sludge filtering time variation can be seen in Figure 3.

In the four variations of the filtering time, the sediment gradually turned cloudy because the high temperature (90 °C) caused a change in solubility, allowing a precipitate to form [25]. The precipitate formed during the heating process is in the form of a brown slurry, which is a $FeCO_3$ compound. The precipitate can be seen at the bottom of the container. It shows that there are still many metal impurities after the precipitation process. As for Ca, although it is not visible visually, the result of the AAS test in Table 2 shows that the process of filtering the stepped filtering has an effect because the element of Ca is also reduced when compared to the precipitation filtrate before post-treatment.

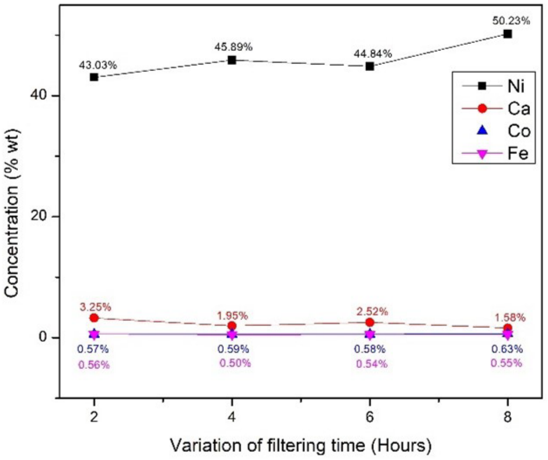

Figure 4: Chemical composition of Fe, Ni, Co, and Ca elements on the crystal products (after crystallization, washing, and drying).

3.2 *Effect of time of stepped filtering sludge on chemical composition of crystals*

XRF testing was carried out to determine the elemental composition of the precipitation product resulting from variations in the time difference of stepped filtering when heating. XRF test results can be seen in Figure 4.

From Figure 4, the trend of nickel content produced tends to increase, inversely proportional to Ca as the most impurity element. However, as for the Fe and Co contained in the crystals, there is no significant difference in the variations carried out.

When compared with the nickel composition trend curve in the AAS test after variation, the nickel composition trend of crystallization results is inversely proportional. It happens because the influence of Ca is reduced when the crystal washing process is carried out. The crystal washing process is carried out to improve the quality of the resulting product by removing unwanted impurities [26]. Washing is done

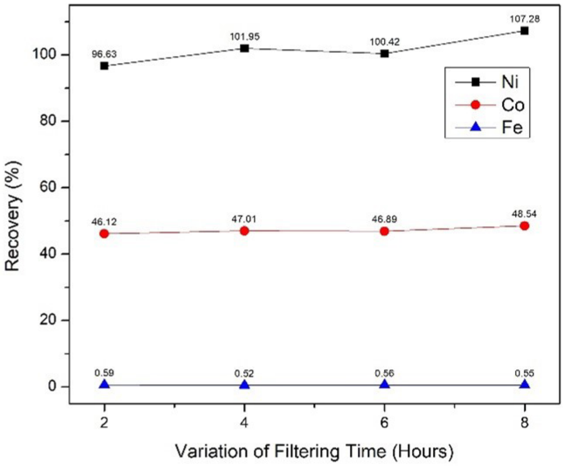

Figure 5: Recovery of Ni, Fe, and Co elements depends on the stepped filtering time variation.

using distilled water because $CaSO_4$ is a compound difficult to dissolve in water, so it tends to settle [27]. Generally, the longer the filtering time will be able to lower the impurities and eventually increase the nickel content in the crystal. However, again, the long time can precipitate impurities in the solution.

The highest nickel composition is found in the 8 h filtration time difference variation with a nickel content of 50.23%. It was obtained because Ca, as the main impurity, decreased due to the washing process with a final composition of 1.58%. The high concentration of Ca most influenced the reduction in Ca at a time variation of 8 h before the washing process was carried out. A higher Ca concentration will form more precipitate so that it can be separated from the filtrate and increase the purity of the resulting crystal. However, based on the XRF test results, the Ca impurity content is still above the threshold for NMC batteries, a maximum of 0.01 wt%. Therefore, in further research, the focus is to reduce the Ca impurity content further. It can be done by adding D2EHPA [28].

3.3 *Effect of time of stepped filtering sludge on recovery*

Figure 5 shows the recovery of each important element in crystal powder after drying. In Figure 5, it can be seen that recovery trends increase as the difference in filtering time increases. It is directly proportional to the composition of Ni contained in the crystallization results. Increased recovery was found in the variation of the difference in filtering time for 8 h. It was obtained because the variation of the 8 h filtering time also resulted in the highest chemical composition of nickel, which affected the recovery.

In Figure 5, it can be seen that recovery trends increase as the difference in filtering time increases. It is directly proportional to the composition of Ni contained in the crystallization results. Increased recovery was found in the variation of the difference in filtering time for 8 h. It was obtained because the variation of the 8 h filtering time also resulted in the highest chemical composition of nickel, which affected the recovery. Powder impurities (possibly $CaSO_4$) or moisture may also cause too high recovery (exceeded 100%). After a series of leaching, precipitation, and stepped filtering processes, the moisture contained in nickel sulfate powder is high. Although it has gone through a drying process, nickel sulfate powder may be able to absorb the moisture around it to form $NiSO_4.6H_2O$ (the XRD test confirms this). In addition, impurities contained in nickel sulfate powder may also absorb the moisture around it (although this is not visible in the XRD test results). The moisture will make the product mass heavier, causing the recovery to be more than 100 %.

3.4 *Effect of time of stepped filtering sludge on separation efficiency*

Grade and recovery values are needed to evaluate the process, but grade and recovery are independent. Separation Efficiency is one of the efforts to combine the value of grade and recovery in mineral processing [29]. Separation Efficiency calculation is carried out to determine which process is better even though each variation has differences in grade and recovery. Based on the Separation Efficiency calculation using Equation (4), the Separation Efficiency results are obtained, as shown in Figure 6.

From Figure 6, the trend value of Separation Efficiency Ni tends to increase as the difference in filtering time increases. The calculation of Separation Efficiency is influenced by grade and recovery values [Equation (4)]. Therefore, the greater the difference recovery of the desired product or valuable mineral and the recovery from gangue, the greater the value of Separation Efficiency obtained. Therefore, the highest

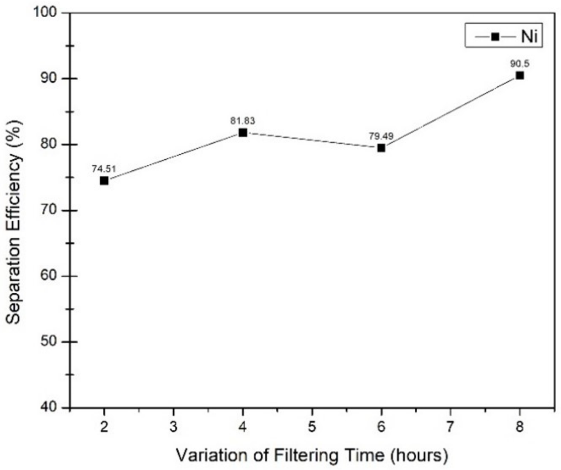

Figure 6: Trend graph of separation efficiency of nickel elements.

Separation Efficiency Ni was obtained at a variation of the filtering time of 8 h because it had the recovery and the least impurities. Also, 8 h of filtering time is still better than the others because the Ni losses are the lowest.

3.5 *Effect of time of stepped filtering sludge on compounds formed*

XRD testing was conducted to determine the compounds formed from the precipitation product. The compounds formed were analyzed by adjusting the peak of the test results with the reference data to be used. The results of the XRD graph for each variation of the filtering time can be seen in Figure 7.

Nickel sulfate hexahydrate compound ($NiSO_4.6H_2O$) is formed in each variation of filtration time when heating. $NiSO_4.6H_2O$ compound is a crystalline form of $NiSO_4$, which is formed due to the crystallization process, when takes place at temperatures above 31.5 °C [30]. $NiSO_4$ is formed in the leaching process, where the NiO compound reacts with H_2SO_4 to form $NiSO_4$. The number of $NiSO_4.6H_2O$ compounds formed is influenced by the amount of nickel-metal dissolved during the leaching process and the increased pH during precipitation [31]. The compound $NiSO_4.6H_2O$ is the target compound that wants to be produced as a product based on Figure 7. Other compounds are formed as impurities. The impurities formed are ferrous sulfate ($FeSO_4$), calcium sulfate ($CaSO_4$), and cobalt sulfate ($CoSO_4$).

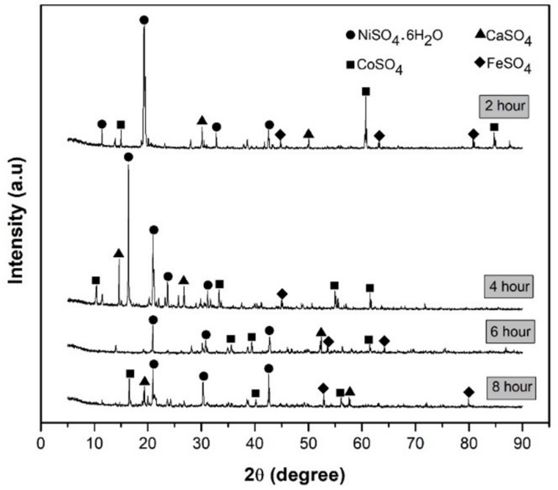

Figure 7: XRD test result for crystal product.

$CoSO_4$ also formed in the leaching according to the reaction in Equation (2). When viewed from the periodic table, nickel and cobalt metals are in proximity. It causes nickel and cobalt metals to be difficult to separate because they have almost the same depositional pH range [32].

$FeSO_4$ compound is formed in the leaching according to Equation (2). In the precipitation process, $FeSO_4$ will react with $CaCO_3$ to form a precipitate of $FeCO_3$. This compound will then be filtered from the solution filtrate. The finding of $FeSO_4$ indicates that the precipitation process is not optimal. $CaSO_4$ compounds are formed during precipitation [Equations (5) and (6)].

$$H_2SO_{4(aq)} + CaCO_{3(s)} \rightarrow CaSO_{4(s)} + H_2O + CO_{2(g)} \quad (5)$$

$$FeSO_{4(aq)} + CaCO_{3(s)} \rightarrow CaSO_{4(s)} + FeCO_{3(s)} \quad (6)$$

4 Conclusions

Nickel sulfate powder can be synthesized from laterite nickel ores by smelting and hydrometallurgical processes. This research focuses on its hydrometallurgical section. After leaching, precipitation, washing, and crystallization processes, nickel sulfate powder can be obtained. The best nickel sulfate powder product was obtained using a stepwise filtering time of 8 h. When using this time, the nickel sulfate product has the highest Nickel content, 50.23%. In addition, using this time, the impurities content is also the smallest compared to the others. The Ca content in powder can be significantly lowered through precipitation, washing, and crystallization processes. Generally, the Ca concentration value can be significantly decreased when the stepping filtering time is varied. It can happen because the solubility continues to decrease as the volume of the solution decreases due to filtration. The highest nickel and cobalt recoveries were also achieved using a stepping filtering time of 8 h. All nickel was recovered after the filtering and leaching process. However, it was found that a recovery exceeded 100%. It may also be due to impurities (probably as $CaSO_4$) or moisture around the powder. For the Separation Efficiency of Ni, the highest value was obtained at the stepping filtering time of 8 h, amounting to 90.50%. In addition, impurities ($CaSO_4$, $FeSO_4$, and $CoSO_4$) are still found in the crystallized product. However, the impurities obtained are also relatively small.

Although it still needs to be eliminated in further research. The $FeSO_4$ and $CoSO_4$ content will likely come from the rest of Ferronickel's leaching and precipitation process. While $CaSO_4$ comes from the pH adjustment stage during the precipitation process. The pH adjustment is made by adding $CaCO_3$ powder. While $CoSO_4$ is an impurity that may provide benefits as a source of Co, which is also needed in the NMC battery manufacturing process. Although the nickel content obtained has reached battery grade, the content of impurities such as iron and calcium that can be achieved in this study is still above the maximum limit of battery grade. Therefore, in future research, it is necessary to modify the precipitation and washing processes.

Acknowledgement

The authors express sincere gratitude to the Ministry of Education, Culture, Research, and Technology of Republik Indonesia which has supported the funding of this research through the Penelitian Tesis Magister Scheme with a research main contract number: 084/E5/PG.02.00.PT/2022 and secondary contract number: 1465/PKS/ITS/2022.

Author Contributions

A.M.F.: investigation, methodology, writing an original draft; Y.S: conceptualization, investigation, reviewing and editing; F.A.: conceptualization, methodology; S.P.: conceptualization, data curation, writing—reviewing and editing, funding acquisition, project administration. All authors have read and agreed to the published version of the manuscript.

Conflicts of Interest

The authors declare no conflict of interest.

References

[1] D. Armstrong McKay, A. Staal, J. Abrams, R. Winkelmann, S. Cornell, I. Fetzer, and T. Lenton, “Global warming of 2 °C risks triggering multiple climate tipping elements,” presented at the AGU Fall Meeting Abstracts, New Orleans, USA, Dec. 13–17, 2021.

[2] D. Liu, L. Xu, U. H. Sadia, and H. Wang, “Evaluating the CO_2 emission reduction effect of China’s battery electric vehicle promotion efforts,” *Atmospheric Pollution Research*, vol. 12, no. 7, Jul. 2021, Art. no. 101115, doi: 10.1016/j.apr.2021.101115.

[3] A. Gomez-Martin, F. Reissig, L. Frankenstein, M. Heidbüchel, M. Winter, T. Placke, and R. Schmuch, “Magnesium substitution in Ni-Rich NMC layered cathodes for high-energy lithium ion batteries,” *Advanced Energy Materials*, vol. 12, no. 8, Feb. 2022, Art. no. 2103045, doi: 10.1002/aenm.202103045.

[4] E. Kartini, M. Fakhrudin, W. Astuti, S. Sumardi, and M. Z. Mubarok, “The study of (Ni,Mn,Co) SO_4 as raw material for NMC precursor in lithium ion battery,” in *the International Conference on Advanced Material and Technology (ICAMT) 2021*, vol. 2708, no. 1, 2022, doi: 10.1063/5.0122596.

[5] F. Abdul, H. V. Suryandaru, N. D. Saputra, and S. Pintowantoro, “The effect of sulfuric acid concentration on the leaching process of crude Fe-Ni obtained from mini blast furnace process,” in *the 4th International Conference on Materials and Metallurgical Engineering and Technology (ICOMMET) 2020*, 2021, vol. 2384, no. 1, doi: 10.1063/5.0071478.

[6] T. Havlík, “Chapter 4 - Equilibrium in Aqueous Solutions,” in *Hydrometallurgy*, T. Havlík, Ed.,

Sawston, England: Woodhead Publishing, pp. 60–95, 2008, doi: 10.1533/9781845694616.60.

[7] C. Shi, X. Zuo, and B. Yan, “Selective recovery of nickel from stainless steel pickling sludge with NH_3-$(NH_4)_2CO_3$ leaching system,” *Environmental Technology*, pp. 1–14, Apr. 2022, doi: 10.1080/09593330.2022.2056085.

[8] S. Yang, P. Zhang, F. Lai, S. Ling, Y. Huang, K. Liu, F. Zheng, H. Wang, X. Zhang, and Q. Li, “New strategy of electrochemical precipitation to metals separation in spent NCM cathode materials for direct regeneration,” *Electrochim Acta*, vol. 431, Nov. 2022, Art. no. 141144, doi: 10.1016/j.electacta.2022.141144.

[9] V. Miettinen, J. Mäkinen, E. Kolehmainen, T. Kravtsov, and L. Rintala, “Iron control in atmospheric acid laterite leaching,” *Minerals*, vol. 9, no. 7, Jun. 2019, Art. no. 404, doi: 10.3390/min9070404.

[10] K. Petkov, V. Stevanova, L. Stamenov, and P. Iliev, “A study of the partial precipitation process of solutions obtained during autoclave dissolution of pyrite concentrate,” *Journal of Chemical Technology and Metallurgy*, vol. 52, no. 2, pp. 270–276, 2017.

[11] L. Cassayre, B. Guzhov, M. Zielinski, and B. Biscans, “Chemical processes for the recovery of valuable metals from spent nickel metal hydride batteries: A review,” *Renewable and Sustainable Energy Reviews*, vol. 170, Dec. 2022, Art. no. 112983, doi: 10.1016/j.rser.2022.112983.

[12] H. Han, W. Sun, Y. Hu, H. Tang, and T. Yue, “Magnetic separation of iron precipitate from nickel sulfate solution by magnetic seeding,” *Hydrometallurgy*, vol. 156, pp. 182–187, Jul. 2015, doi: 10.1016/j.hydromet.2015.07.001.

[13] H. Han, W. Sun, Y. Hu, T. Yue, L. Wang, R. Liu, Z. Gao, and P. Chen, “Induced crystallization of goethite precipitate from nickel sulfate solution by limonite seeding,” *Hydrometallurgy*, vol. 174, pp. 253–257, Dec. 2017, doi: 10.1016/j.hydromet.2017.03.001.

[14] Z. T. Ichlas, M. Z. Mubarok, A. Magnalita, J. Vaughan, and A. T. Sugiarto, “Processing mixed nickel cobalt hydroxide precipitate by sulfuric acid leaching followed by selective oxidative precipitation of cobalt and manganese,” *Hydrometallurgy*, vol. 191, Jan. 2020, Art. no. 105185, doi: 10.1016/j.hydromet.2019.105185.

[15] O. A. Nasser and M. Petranikova, “Review of achieved purities after li-ion batteries hydrometallurgical treatment and impurities effects on the cathode performance,” *Batteries*, vol. 7, no. 3, Sep. 2021, Art. no. 60, doi: 10.3390/batteries7030060.

[16] N. Pandey, S. K. Tripathy, S. K. Patra, and G. Jha, “Recent Progress in hydrometallurgical processing of nickel lateritic ore,” *Transactions of the Indian Institute of Metals*, vol. 76, no. 1, pp. 11–30, Jan. 2023, doi: 10.1007/s12666-022-02706-2.

[17] S. Pintowantoro, P. C. Panggabean, Y. Setiyorini, and F. Abdul, “Smelting and selective reduction of limonitic laterite ore in mini blast furnace,” *Journal of The Institution of Engineers (India): Series D*, vol. 103, no. 2, pp. 591–600, Dec. 2022, doi: 10.1007/s40033-022-00348-8.

[18] F. Abdul, S. Pintowantoro, and A. Maulidani, “Analysis the effect of charcoal mass variation to Ni content, sinter strength and yield on sintering process of limonitic laterite nickel ore,” *Key Engineering Materials*, vol. 867, pp. 25–31, Oct. 2020, doi: 10.4028/www.scientific.net/KEM.867.25.

[19] S. Pintowantoro, K. Oktandria, R. A. M. Pasha, and F. Abdul, “Variation of oxygen flow rate on nickel and iron content in the oxidation refining process of crude Fe-Ni from Mini Blast Furnace (MBF),” in *the 4th International Conference on Materials and Metallurgical Engineering and Technology (ICOMMET) 2020*, vol. 2384, no. 1, 2021, doi: 10.1063/5.0071487.

[20] S. Pintowantoro, F. Waluyo, Y. Setiyorini, V. Setyowati, A. Kawigraha, and F. Abdul, “Study of the effect of time variations on the leaching process of ferronickel products from mini blast furnace to yield elements of Fe, Ni, and Co for $NiSO_4.6H_2O$ Synthesis,” *Journal of Physics*, vol. 2117, no. 1, Nov. 2021, Art. no. 012024, doi: 10.1088/1742-6596/2117/1/012024.

[21] B. A. Wills and J. A. Finch, “Introductionin Wills’ Mineral Processing Technology,” *Elsevier*, 2016, pp. 1–27. doi: 10.1016/B978-0-08-097053-0.00001-7.

[22] H. E. Farrah, G. A. Lawrance, and E. J. Wanless, “Solubility of calcium sulfate salts in acidic

manganese sulfate solutions from 30 to 105 °C," *Hydrometallurgy*, vol. 86, no. 1–2, pp. 13–21, Apr. 2007, doi: 10.1016/j.hydromet.2006.10.003.

[23] G. P. Demopoulos, "Aqueous precipitation and crystallization for the production of particulate solids with desired properties," *Hydrometallurgy*, vol. 96, no. 3, pp. 199–214, Apr. 2009, doi: 10.1016/j.hydromet.2008.10.004.

[24] A. J. Bard and L. R. Faulkner, *Electrochemical Methods: Fundamentals and Applications*. New York: Wiley, 1980.

[25] G. Azimi and V. G. Papangelakis, "Thermodynamic modeling and experimental measurement of calcium sulfate in complex aqueous solutions," *Fluid Phase Equilibria*, vol. 290, no. 1–2, pp. 88–94, Mar. 2010, doi: 10.1016/j.fluid.2009.09.023.

[26] B. Padh, P. C. Rout, G. K. Mishra, K. R. Suresh, and B. R. Reddy, "Recovery of nickel and molybdate from ammoniacal leach liquors of spent HDS catalysts using chelating ion exchange resin," *Hydrometallurgy*, vol. 184, pp. 88–94, Mar. 2019, doi: 10.1016/j.hydromet.2019.01.001.

[27] F. Wirsching, "Calcium Sulfate," in *Ullmann's Encyclopedia of Industrial Chemistry*. Weinheim, Germany: Wiley-VCH Verlag GmbH & Co. KGaA, 2000. doi: 10.1002/14356007.a04_555.

[28] L. M. Roux, E. Minnaar, P. J. Cilliers, M. Bellino, and R. Dye, "Comparison of solvent extraction and selective precipitation for the purification of cobalt electrolytes at the Luilu refinery, DRC," in *The South African Institute of Mining and Metallurgy Base Metal Conference*, pp. 343–364, 2007.

[29] B. A. Wills and T. Napier-Munn, "Introduction," in *Wills' Mineral Processing Technology*. Amsterdam, Netherlands: Elsevier, 2005, pp. 1–29, doi: 10.1016/B978- 075064450-1/50003-5.

[30] V. Yu. Gus'kov, D. A. Allayarova, G. Z. Garipova, and I. N. Pavlova, "Supramolecular chiral surface of nickel sulfate hexahydrate crystals and its ability to chirally recognize enantiomers by adsorption data," *New Journal of Chemistry*, vol. 44, no. 41, pp. 17769–17779, 2020, doi: 10.1039/D0NJ03912H.

[31] Z. Zhu, Y. Pranolo, W. Zhang, W. Wang, and C. Y. Cheng, "Precipitation of impurities from synthetic laterite leach solutions," *Hydrometallurgy*, vol. 104, no. 1, pp. 81–85, Jul. 2010, doi: 10.1016/j.hydromet.2010.05.003.

[32] W. Xiao, X. Liu, and Z. Zhao, "Kinetics of nickel leaching from low-nickel matte in sulfuric acid solution under atmospheric pressure," *Hydrometallurgy*, vol. 194, p. 105353, Jun. 2020, doi: 10.1016/j.hydromet.2020.105353.